Balloon Flight Background Measurement with Actively-Shielded Planar and Imaging CZT Detectors

P. F. Bloser[a], T. Narita[b], J. A. Jenkins[b], M. Perrin[c], R. Murray[b], and J. E. Grindlay[b]

[a]Max-Planck-Institut für extraterrestrische Physik, Giessenbachstrasse, D-85748 Garching, Germany

[b]Harvard-Smithsonian Center for Astrophysics, 60 Garden St., Cambridge, MA 02138, USA

[c]Astronomy Department, University of California at Berkeley, Berkeley, CA 94720, USA

ABSTRACT

We present results from the flight of two prototype CZT detectors on a scientific balloon payload in September 2000. The first detector, referred to as "CZT1," consisted of a 10 mm $\times$ 10 mm $\times$ 2 mm CZT crystal with a single gold planar electrode readout. This detector was shielded by a combination of a passive collimator in the front, giving a 40 degree field of view and surrounded by plastic scintillator, and a thick BGO crystal in the rear. The second detector, "CZT2," comprised two 10 mm $\times$ 10 mm $\times$ 5 mm CZT crystals, one made of eV Products high pressure Bridgman material and the other of IMARAD horizontal Bridgman material, each fashioned with a 4 $\times$ 4 array of gold pixels on a 2.5 mm pitch. The pixellated detectors were flip-chip-mounted side by side and read out by a 32-channel ASIC. This detector was also shielded by a passive/plastic collimator in the front, but used only additional passive/plastic shielding in the rear. Both experiments were flown from Ft. Sumner, NM on September 19, 2000 on a 24 hour balloon flight. Both instruments performed well. CZT1 recorded a non-vetoed background level at 100 keV of $\sim 1 \times 10^{-3}$ cts cm^{-2} s^{-1} keV^{-1}. Raising the BGO threshold from 50 keV to $\sim$ 1 MeV produced only an 18% increase in this level. CZT2 recorded a background at 100 keV of $\sim 4 \times 10^{-3}$ cts cm^{-2} s^{-1} keV^{-1} in the eV Products detector and $\sim 6 \times 10^{-3}$ cts cm^{-2} s^{-1} keV^{-1} in the IMARAD detector, a difference possibly due to our internal background subtracting procedure. Both CZT1 and CZT2 spectra were in basic agreement with Monte Carlo simulations, though both recorded systematically higher count rates at high energy than predicted. No lines were observed, indicating that neutron capture reactions, at least those producing decay lines at a few 100 keV, are not significant components of the CZT background. Comparison of the CZT1 and CZT2 spectra indicates that passive/plastic shielding may provide adequately low background levels for many applications.

Keywords: CZT, background, shielding, balloon flights, hard X-ray astronomy, instrumentation

1. INTRODUCTION

Hard X-ray and gamma-ray detectors for high energy astronomy made of Cadmium-Zinc-Telluride (CZT) are finally realizing the potential that they have shown for the past 6–7 years. It has long been known that CZT detectors offer far better energy resolution than scintillator detectors such as NaI and CsI, and that the use of pixel or strip electrode readouts allows far better spatial resolution. Response up to 600 keV is possible with moderate thicknesses (5 mm) due to the high stopping power of CZT, and no cryogenic cooling is required due to its wide band gap. Extensive laboratory work by our group at Harvard[1–4] and many others has now begun to bring this promise to fruition. In the hard X-ray band ($\sim$ 10 to several 100 keV) the first space-based astronomical instrument employing CZT, the Swift mission,[5] is already under construction. EXIST,[6] a wide-field, all-sky survey telescope operating between $\sim$ 5 and 600 keV, is in the early planning stages, and the Hard X-ray Telescope of Constellation-X,[7] a narrow-field instrument using focusing optics up to 40 keV, is under development. CZT is also being considered for the medium gamma-ray band (0.5–50 MeV) as the calorimeter material in advanced Compton telescopes.[8]

Further author information: (Send correspondence to P. Bloser)
P.B.: E-mail: bloser@mpe.mpg.de

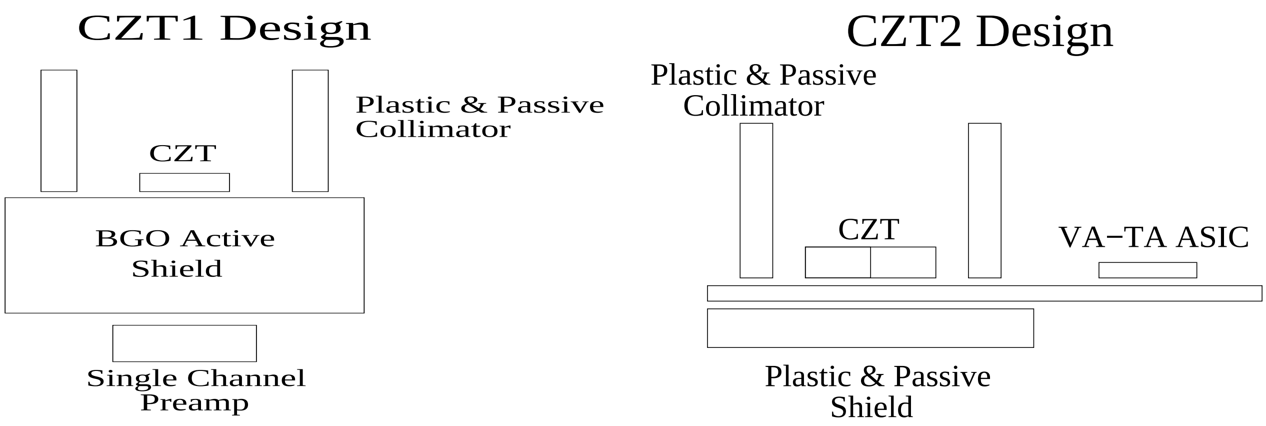

Figure 1. Schematic diagrams of the CZT1 (*left*) and CZT2 (*right*) detectors flown in September 2000. CZT1 is a single-element detector with a passive/plastic collimator and a rear BGO active photon shield. CZT2 consists of two pixellated detectors read out by an ASIC in an identical passive/plastic collimator, but with only additional passive/plastic shielding to the rear.

A major contributor to the maturity of CZT detector technology has been an active campaign of balloon flight tests over the past five years, both by our group[9–11] and by others.[12–16] These experiments are necessary to test detector design, readout, and shielding methods under flight conditions, and to measure background levels in the space environment. The experiments have progressed from simple one-element detectors with passive shielding[12,13] to single-element detectors with various combinations of active and passive shielding[9,12] to complex multi-anode detectors, either strips[14–16] or pixels,[10,11] again using both passive and active shielding techniques. The general conclusions that may be drawn from this experience are that CZT detector technology is indeed compatible with the needs of balloon and space-flight systems, and that background levels can be made acceptable for sensitive astronomical observations. More specifically, active shielding has been shown to reduce background significantly over passive shielding alone.[12,14,15] This suggests a substantial portion of the CZT background is generated by processes involving charged particles and/or prompt gamma reactions. It has been suggested that prompt (n,γ) reactions in CZT could be an important source of background due to the large neutron capture cross sections in Cd.[12,13] Additionally, activation of Cd and Te by neutrons could produce isomeric states that decay radiatively on a timescale too long to be vetoed by active shields.[13] However, flight results with a strip detector from Washington University, St. Louis and the University of California, San Diego (WUSTL/UCSD) saw no evidence of decay lines.[14] In addition, the WUSTL/UCSD experiment found that a shield threshold of 10 MeV, too high to veto prompt gamma-rays, still reduced background to acceptable levels.[15] Perhaps, then, only charged particle shields made out of plastic scintillator are necessary, instead of heavier gamma-ray shields such as CsI or BGO.

In this paper we present results from two CZT experiments conducted in September 2000: the first array of pixellated CZT detectors, read out by an ASIC, to be flown on a balloon, and a single-element background experiment flown simultaneously. Motivated by the requirements of the EXIST concept,[6] our goals were to investigate techniques for assembling a large-area detector plane out of small elements, test various detector materials in the near-space environment, demonstrate an ASIC readout system in flight, and compare active shielding techniques using particle and photon shields for a wide field-of-view telescope.

2. DESCRIPTION OF THE CZT EXPERIMENTS

The motivations for our two experiments and the detector designs have been described in detail previously.[10,11] Here we repeat the main features, as shown schematically in Figure 1.

The first CZT experiment, dubbed "CZT1," is a modification of the CZT/BGO detector flown by us in 1997.[9] Its main purpose was to test the effectiveness of photon vs. particle-only shielding in a wide field of view (FOV) instrument. CZT1 consists of a single-element detector, 10 mm $\times$ 10 mm $\times$ 2 mm, supplied by eV Products and made from high-pressure Bridgman (HPB) material with planar gold contacts. The detector sits directly in front of a thick BGO crystal, 8.2 cm diameter $\times$ 6.5 cm thick, which acts as an active shield. The threshold of the BGO was alternated between $\sim$ 50 keV and $\sim$ 1 MeV to simulate photon and particle rejection, respectively. The CZT is surrounded by a graded Pb-Sb-Cu collimator (4.5 mm Pb, 1 mm Sn, 1 mm Cu) that provides a 40° FOV, appropriate to an all-sky survey telescope such as EXIST. This passive collimator is in turn surrounded by 0.5" thick NE-102 plastic scintillator, read out by miniature PMTs, to reject local gamma production. Only one readout channel was available in addition to the CZT channel, and so the signals from the BGO and the passive/plastic collimator were combined into a single veto.

The second experiment, "CZT2," was intended to test technological requirements for the EXIST concept and to provide a particle-only shielding configuration to compare with CZT1. CZT2 consists of a tiled "array" of two flip-chip-mounted pixellated detectors, each 10 mm $\times$ 10 mm $\times$ 5 mm. One detector is made of HPB CZT provided by eV Products, and the other is horizontal Bridgman (HB) material produced by IMARAD Imaging Systems.[17] Our work with IMARAD HB CZT has shown that is is more uniform than HPB material, and that simple gold contacts greatly reduce leakage current to levels similar to HPB values.[3,4] Both detectors were fashioned with a 4 $\times$ 4 array of gold pixels on a 2.5 mm pitch plus a guard ring; the layout was such that the pitch is preserved across the two tiled detectors. The detectors are mounted side-by-side in a flip-chip fashion on a ceramic carrier board and read out by a self-triggering, 32-channel VA-TA ASIC supplied by IDE Corp. A passive/plastic collimator identical to that in CZT1 provides a 40° FOV. Unlike CZT1, however, CZT2 is shielded from the rear by a simple passive/plastic shield. A weak ^{241}Am source placed just above the collimator supplied in-flight calibration at 60 keV.

3. BALLOON FLIGHT RESULTS

Both the CZT1 and CZT2 experiments were launched on September 19, 2000 from Ft. Sumner, NM as part of a multi-experiment balloon payload that also included Harvard's EXITE2 hard X-ray telescope and MSFC's hard X-ray focusing optics experiment HERO. The flight was quite successful, achieving 24 hours at float altitudes between 115,000 ft and 128,000 ft. The CZT1 detector was intermittently noisy, possibly due to pickup in the plastic shield PMT preamps, and care was taken to extract periods of clean operation as judged by the total count rate. CZT2 performed well throughout the flight.

3.1. CZT1 Results

The September 2000 flight spectrum recorded by the CZT1 experiment is shown in Figure 2. Plotted are both the total and "good," or non-vetoed, events. Data are included from the entire flight, as no altitude-dependent variations within the range of float altitudes was found previously.[9] Plotted separately are 5.8 hours of data with the BGO threshold set at $\sim$ 50 keV (closed symbols) and 3.3 hours of data with the BGO threshold set at $\sim$ 1 MeV (open symbols). Also shown for reference are the background levels recorded by the same detector as part of the CZT/BGO experiment flown in 1997.[9]

It is immediately clear that the 2000 background is in very good agreement with the background recorded in 1997 except at energies below $\sim$ 100 keV, where the larger aperture flux seen in the 40° FOV is apparent. In 1997 the CZT detector was completely covered by a graded Pb-Sn-Cu cup to approximate the grammage of a collimator. At 100 keV the measured good event level in the 2000 data, for a BGO threshold of 50 keV, is $\sim 1 \times 10^{-3}$ cts cm^{-2} s^{-1} keV^{-1}. The BGO provides a factor of $\sim$ 4.5 reduction at this energy, again showing that active shielding is essential. What is also noteworthy is that the background level at 100 keV increases by only $\sim$ 18% when the BGO threshold is increased to 1 MeV. The increase is approximately constant at all energies. This confirms the previously-reported result that active photon shields may be replaced with lighter plastic charged particle shields with only a small penalty in background rate.[15]

3.2. CZT2 Results

3.2.1. In-flight Detector Performance

One of the primary goals for CZT2 was to demonstrate the in-flight performance of two pixellated CZT detectors read out by an ASIC. Although more than half of the channels of the IMARAD detector were unusable due to bad

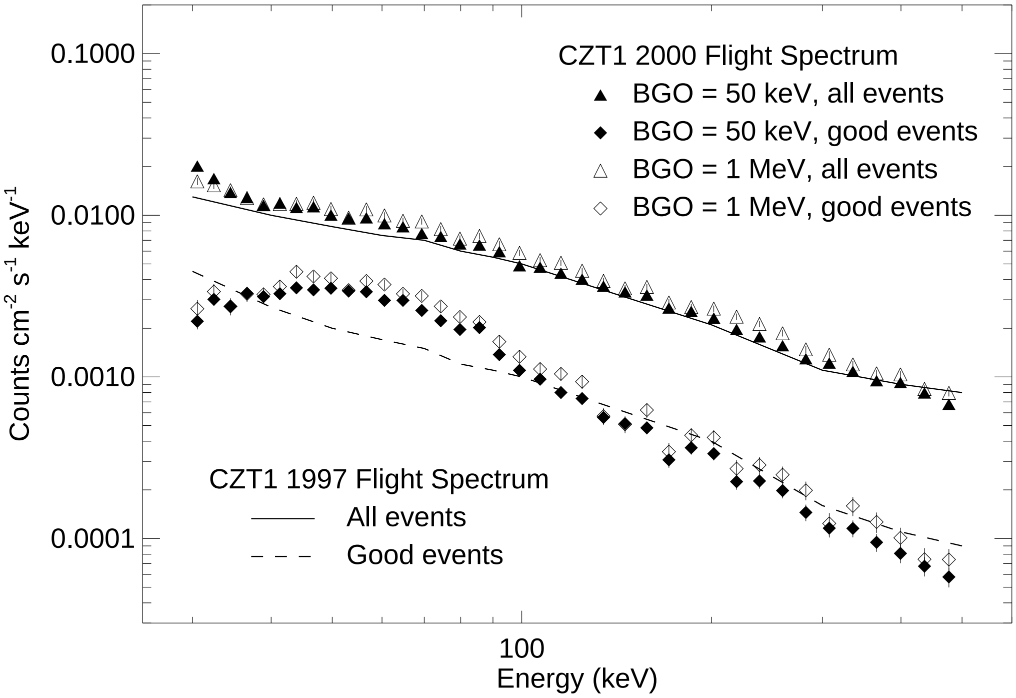

Figure 2. Background spectrum recorded by the CZT1 experiment during the September 2000 flight. Shown are both total and "good" events for BGO threshold settings of 50 keV (closed symbols) and 1 MeV (open symbols). The background level at 100 keV for the lower BGO threshold setting is $\sim 1 \times 10^{-3}$ cts cm^{-2} s^{-1} keV^{-1}. At the higher BGO threshold the background at 100 keV increases by $\sim$ 18%. Also plotted are the total and good background levels recorded by the 1997 CZT/BGO experiment.[9]

contacts after flip-chip mounting or noise from long lead lengths,[11] a few of the IMARAD HB CZT pixels and all of the eV Products HPB CZT pixels functioned properly. (The functioning IMARAD pixels, unfortunately, happened to correspond to areas of the detector with poor material qualities.[11]) The performance may be judged by the spectra recorded from the ^{241}Am calibration source. An example from each detector is presented in Figure 3. Both spectra were corrected for the effects of charge spreading by adding in charge from the nearest-neighbor pixel, as described previously.[11] The improvement in the spectra is clear. The spectra were fit with a combination of a gaussian photopeak and exponential tail to determine energy resolution and photopeak efficiency, where the photopeak efficiency is defined as the ratio of photopeak counts to total counts within a range around the gaussian center from -4σ to $+2.35\sigma$.[2] At left is an IMARAD pixel with an energy resolution (corrected spectrum) of 13.3% at 60 keV and a photopeak efficiency of 85%. At right is an eV Products pixel with an energy resolution of 9.4% and a photopeak efficiency of 92%. While the photopeak efficiencies are consistent with those measured on the ground, the energy resolutions are slightly worse; at 60 keV we measured 12.9% for the IMARAD pixel and 8.5% for the eV Products pixel in pre-flight calibrations. The degradation is small, however. We conclude that a pixellated detector with ASIC readout may be made to function properly under spaceflight conditions.

3.2.2. Temperature Effects

A temperature sensor was included in the CZT2 experiment to monitor the sensitivity of the detector gain, offset, and noise to temperature. During the course of the flight the temperature inside the CZT2 pressure vessel varied between 10 °C and 31 °C. The CZT2 data were assembled into 30 minute segments, and the peak channel and width σ of both the ^{241}Am line and the offset pedestal peak were determined for an arbitrary channel for each

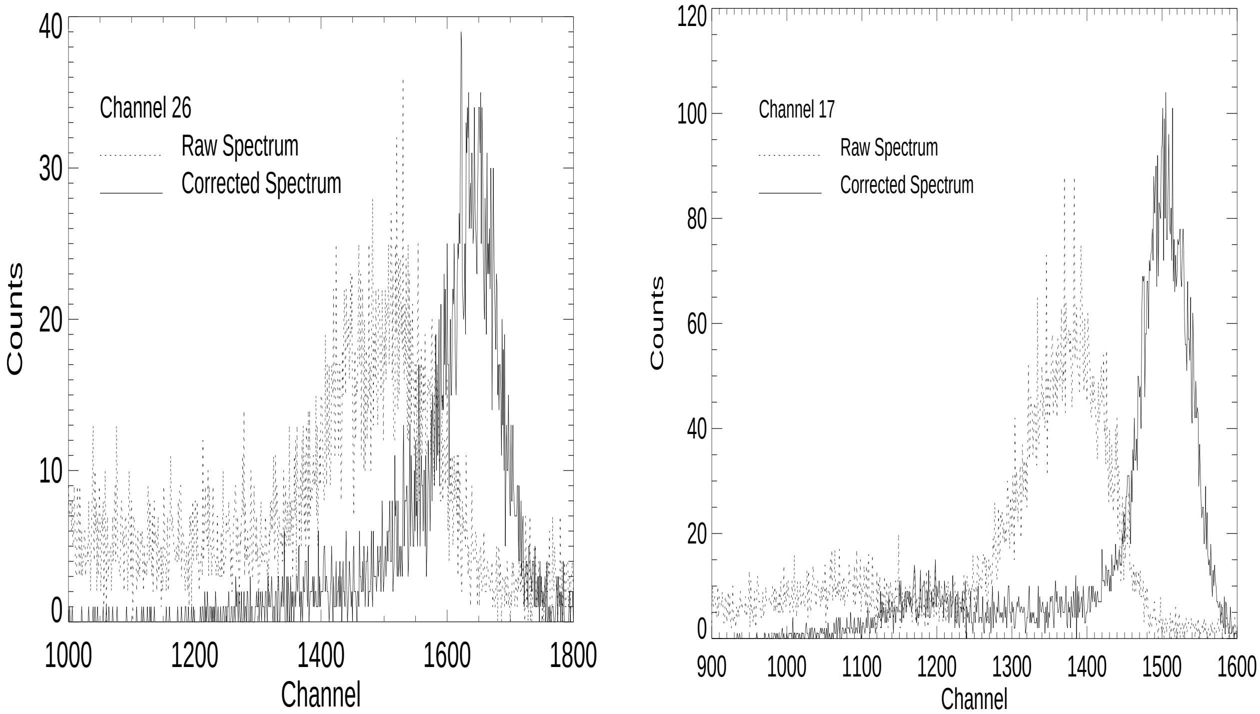

Figure 3. In-flight spectra of the ^{241}Am 60 keV calibration source, showing the improvement achieved by adding charge from nearest-neighbor pixels. At left is a pixel from the IMARAD HB CZT detector, with a corrected energy resolution of 13.3% and a photopeak efficiency of 85%. At right is a pixel from the eV Products HPB CZT detector, with an energy resolution of 9.4% and a photopeak efficiency of 92%. While the photopeak efficiencies are consistent with those measured on the ground, the energy resolutions are slightly worse.

segment. Scatter plots of these quantities revealed no correlation between the width σ of the line or pedestal and the temperature. There is, however, a strong correlation with temperature for the peak channel of both the ^{241}Am line and the pedestal. In Figure 4 we show scatter plots of the ^{241}Am peak vs. temperature (left) and the difference between the ^{241}Am peak and the pedestal peak vs. temperature (right). The line peaks are expressed in keV using the pre-flight energy calibration. It is clear that the calibration has changed in flight, and that this change is highly correlated with the temperature; the ^{241}Am line moves between 54 keV and 58.5 keV within this temperature range. However, the difference between the line peak and the pedestal peak, though also correlated with temperature, changes far less, only by about 1 keV. (Note that according to our pre-flight energy calibrations, which made use of three different line energies, the pedestal peak is not located exactly at 0 keV.) This indicates that it is the offset, rather than the gain, that is most affected by the temperature. This means that, to first order, we may correct the energy of the in-flight spectra by a simple shift in energy offset. It does indicate, however, that some degree of temperature control or electronic offset correction should be developed for stable operation under flight conditions.

3.2.3. Background Spectrum

In processing the CZT2 flight data it was immediately clear that the recorded background spectra were much flatter than expected, failing to fall off appreciably at high energy. This was true also of the IMARAD pixels that had been masked out due to their high noise: instead of just a low energy noise peak, as expected, the masked pixels also had recorded a flat spectrum extending to high energies. This was probably due to cosmic ray events producing multiple triggers in the ASIC, as we had no upper level discriminator implemented. To produce

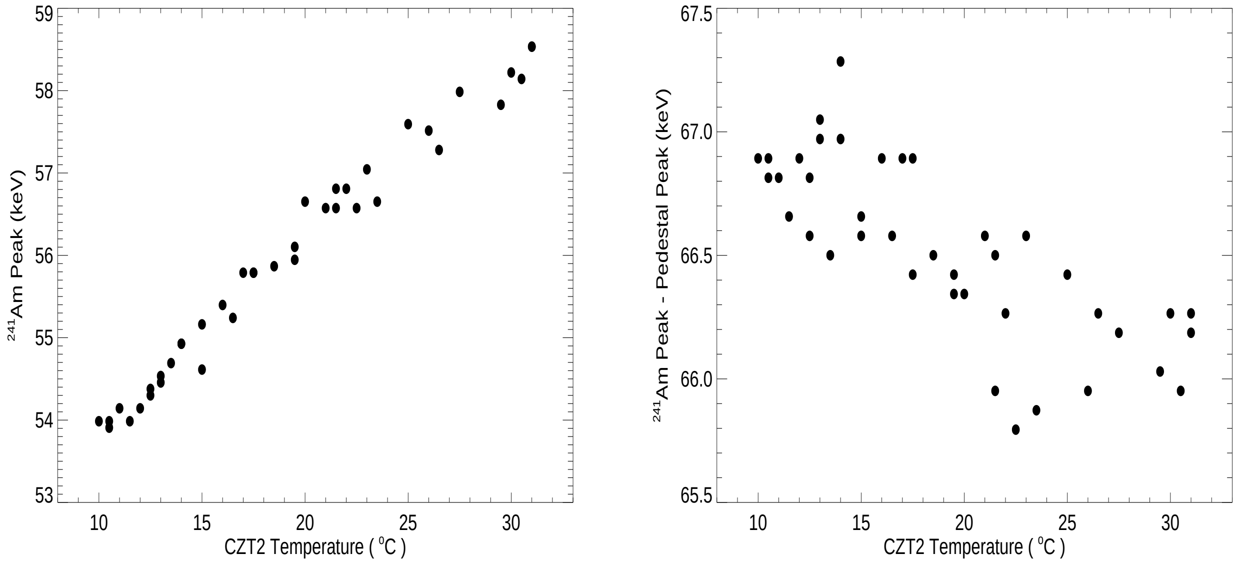

Figure 4. Scatter plots showing the relation between the ^{241}Am line peak and the temperature (*left*), and the difference between the ^{241}Am peak and the pedestal peak and the temperature (*right*). The line peaks are expressed in energy using the pre-flight calibration. There is clearly a very strong correlation between the temperature and the channel of the 60 keV peak. The difference between the ^{241}Am peak and the pedestal peak changes by a much smaller amount, however, indicating that it is the offset, rather than the gain, that is strongly dependent on the temperature.

accurate background spectra we therefore averaged the masked pixels into a "masked background" spectrum and subtracted this from the spectra of the active pixels. The masked pixels were unfortunately all located on the IMARAD detector, so that it is not clear that this masked background is appropriate for the eV Products detector; the resulting spectra from the two detectors agree reasonably well up to their normalization, however (see below), so we do not believe this has had a big effect on our results. In order to compare these results with future data from the CZT3 detector, which will employ an ASIC which provides only the peak channel for each event (see separate paper in these proceedings), we have not added in charge from neighboring pixels in producing the CZT2 background spectra.

The September 2000 flight spectra recorded by the CZT2 experiment are shown in Figure 5. Plotted are total and good (non-vetoed by the plastic shields) events for both the eV Products HPB detector and the IMARAD HB detector. A total of 4.9 hours of data is included, during which time the temperature increased from 10 °C to 17 °C. From Figure 4 we expect the offset to vary by less than 2 keV and the gain by less than 0.5 keV over this range. Due to the coarse binning used for the background continuum spectra we have not made these small corrections; rather, the individual spectra were simply shifted in energy by 4–5 keV so that the ^{241}Am calibration lines were superimposed at 60 keV. The spectra represent the average of all pixels in each detector with similar response and material quality (10 pixels from the eV Products detector and 3 pixels from the IMARAD detector), as judged by the ^{241}Am calibration line. Due to the slight line broadening in flight noted in Section 3.2.1 it was difficult to cleanly subtract the calibration line profile, recorded on the ground, from the flight background spectra. We have therefore excluded events between 42 keV and 67 keV from the spectra shown.

The CZT2 spectra presented in Figure 5 show that simple passive and plastic shielding can reduce background in CZT detectors to reasonable levels. The background recorded at 100 keV is $\sim 4\times10^{-3}$ cts cm^{-2} s^{-1} keV^{-1} for the eV Products detector and $\sim 6\times10^{-3}$ cts cm^{-2} s^{-1} keV^{-1} for the IMARAD detector. The spectra overall agree in shape and normalization to within a factor of $\sim$ 2. The difference in normalization could well arise from using the IMARAD masked pixel background for the eV Products crystal. In both cases the plastic shield vetoes reduce the background by a factor of $\sim$ 2–2.5. Also notable is the lack of any detected background

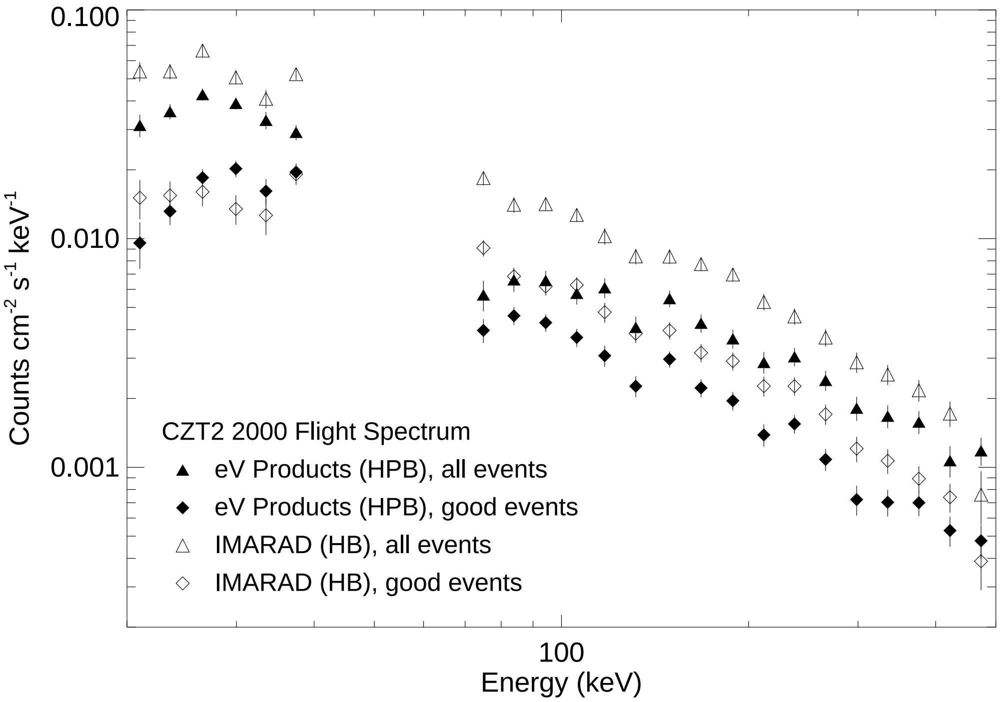

Figure 5. Background spectra recorded by the CZT2 experiment during the September 2000 flight. Shown are both total and good events for the eV Products (HPB CZT) detector (closed symbols) and the IMARAD (HB CZT) detector (open symbols). The background level at 100 keV is $\sim 4 \times 10^{-3}$ cts cm^{-2} s^{-1} keV^{-1} for the eV Products detector and $\sim 6 \times 10^{-3}$ cts cm^{-2} s^{-1} keV^{-1} for the IMARAD detector. In both cases the plastic shield vetoes reduce the background by a factor of $\sim$ 2–2.5. Events between 42 keV and 67 keV have been excluded due to poor subtraction of the 60 keV ^{241}Am calibration line.

lines, which a pixellated detector should be able to resolve. This is in agreement with the findings of the WUSTL/UCSD experiment,[14] which used crossed strips to achieve energy resolution similar to that of a pixel detector. These findings cast doubt on the importance of activation lines from neutron interactions as a source of CZT background,[12,13] at least for lines below $\sim$ 500 keV.

3.3. Comparison of CZT1 and CZT2 Results

In Figure 6 we compare the flight spectra recorded by CZT1 and CZT2, plotted as count rate per volume to account for the different detector thicknesses. Both CZT2 detectors are plotted, as are CZT1 results for both BGO threshold settings. The agreement below 100 keV is quite good. At higher energies the CZT2 spectra are flatter, reaching up to a factor of $\sim$ 4 higher than the CZT1 spectra. This is not surprising; clearly the large BGO crystal is more effective at shielding the small CZT1 detector than plastic, even at a threshold of 1 MeV. CZT2 also unavoidably had passive material in its field of view, which might contribute to the difference as well. However, the relatively modest increase in background for CZT2 with passive/plastic shielding only may be a small price to pay compared to the savings in space and mass achieved with thin, light plastic scintillator shields, especially for large, wide-angle, coded-mask survey telescopes. These results again support the findings of the WUSTL/UCSD experiment.[15]

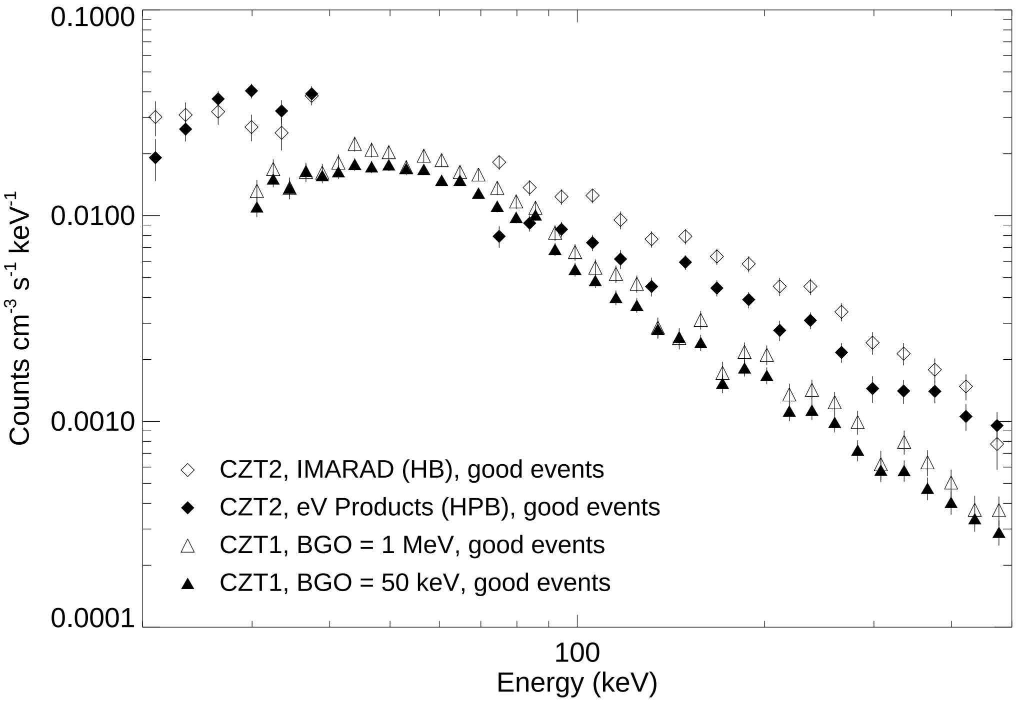

Figure 6. Comparison of CZT1 and CZT2 results. Here the background per unit volume is presented due to the different detector thicknesses. Both CZT2 detectors are shown, as is the CZT1 rate for both BGO threshold settings. At high energies the CZT1 background is up to a factor of ~ 4 lower than the CZT2 background, presumably due to the large BGO active shield. This difference is relatively modest, however, and the far lower mass of plastic shielding may make this a worthwhile tradeoff for many applications.

4. DETECTOR SIMULATIONS AND PREDICTED BACKGROUND

We have attempted to reproduce the results of both CZT experiments using Monte Carlo simulations conducted with MGEANT,[18] an improved user interface to the standard CERN Program Library simulation package GEANT. Mass models of both CZT1 and CZT2 were constructed and illuminated with parameterizations of the atmospheric gamma-ray spectrum,[19] cosmic ray proton spectrum,[20] and atmospheric neutron spectrum.[20,21] These input spectra were assumed to be isotropic for simplicity, and are generally accepted to be accurate to about a factor of 2. The location and energy deposit of all interactions in the CZT and shields were recorded. The CZT energy deposits were then modified to take into account the response of the detectors. For CZT1, a planar detector, this was done simply according to the Hecht relation[22] using charge transport values of $\mu_e\tau_e = 5 \times 10^{-3}$ cm^2 V^{-1} and $\mu_h\tau_h = 3 \times 10^{-5}$cm^2 V^{-1}.[9] For CZT2 the deposited charge was propagated according to the applied electric field and the induced signal calculated from the weighting potential; we used $\mu_e\tau_e = 3 \times 10^{-3}$ cm^2 V^{-1} and $\mu_h\tau_h = 10^{-6}$cm^2 V^{-1}.[11] These $\mu\tau$ values were derived for each detector by matching simulated line spectra to recorded line spectra. The resulting spectra were convolved with the measured energy resolution of each detector.

The good event flight spectrum of CZT1 (with a BGO threshold of 50 keV) is compared to the MGEANT simulation in Figure 7. In the simulation all proton-induced events were vetoed by the plastic and BGO and the neutron component was negligible (see below), so only the gamma-ray component is shown. Although the simulations agree with the data near 100 keV, it is clear that the overall shape is not well-reproduced. At high energies the simulations fail to reproduce the recorded counts by a factor of 2–3, much the same as in the 1997 flight.[9] Given the large uncertainties in the input atmospheric gamma-ray spectrum, this is not too surprising.

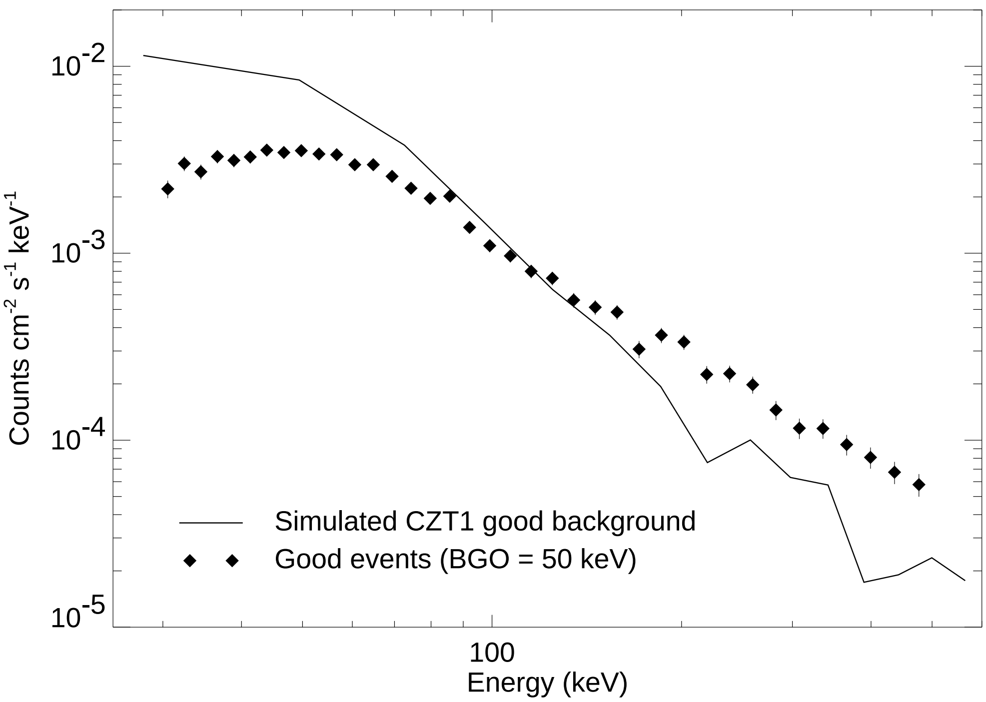

Figure 7. CZT1 Good event flight spectrum (BGO threshold = 50 keV) compared to MGEANT simulation. Only gamma-ray-induced events are included, as the simulated contribution from protons was completely vetoed by the plastic and BGO shields. At high energies, the simulation fails to reproduce the recorded counts, much the same as in the 1997 flight.[9] At low energies the predicted level of aperture flux is not seen, perhaps due to shielding of the CZT by the gondola structure (not included in the simulations).

At low energies the predicted aperture flux, enhanced by the Hecht relation, is not observed, perhaps due to shielding by the gondola structure (which was not included in the simulation due to its size and complexity). The CZT1 instrument was bolted to the main EXITE2 elevation flange next to an electronics rack, both sizable pieces of aluminum, and it is possible that cosmic ray or neutron-induced background in this structure contribute to the higher-than-predicted count rate at high energies.

In Figure 8 we compare the measured CZT2 flight spectra to the MGEANT simulation. We show separately the predicted background generated by atmospheric gamma-rays, both via aperture flux and shield leakage, and the background from cosmic ray proton interactions. The contributions from atmospheric neutrons were again negligible. We note that accurate simulations of neutron-generated background are notoriously difficult to perform,[13] and that the standard MGEANT-GCALOR setup we used is probably too simplistic to be believable without very careful attention to the precise isotopic composition of the detectors and surrounding materials. The combined photon and proton simulated spectra agree with the data to within a factor of ~ 2, falling systematically shy of the mark at high energies as in CZT1. The CZT2 experiment was surrounded by extensive gondola and detector structures, and background generated in these could play a role in the flatter observed spectrum. We did take care to include two thick pieces of aluminum in the CZT2 field of view. We note that, although no lines are seen below 500 keV, higher-energy neutron activation lines cannot be excluded, and these would form a Compton continuum in the CZT which might account for the higher-than-predicted high energy background in both CZT1 and CZT2. Considering the uncertainty in the input spectra, however, we consider the general level of agreement between the data and simulations to be satisfactory.

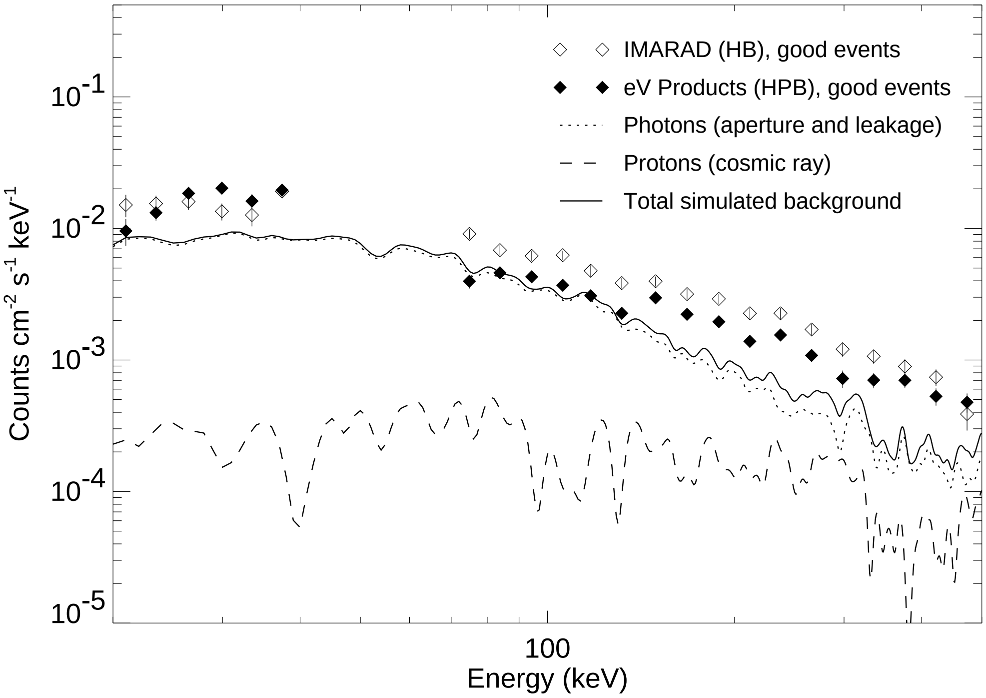

Figure 8. CZT2 flight spectra (eV Products and IMARAD detectors) compared to the MGEANT simulations. Included are the predicted spectra from aperture photons, shield leakage photons, and cosmic ray proton interactions. The contribution from atmospheric neutrons was found to be negligible, although the standard MGEANT-GCALOR setup is probably too simplistic to be realistic. The jagged structure in the proton spectrum is due to poor statistics convolved with the detector energy resolution. The data and simulation agree to within a factor of ~ 2, although the recorded spectrum is systematically flatter at high energies, as in CZT1.

5. CONCLUSIONS AND FUTURE WORK

We have successfully flown two CZT detector experiments, dubbed CZT1 and CZT2, that have provided valuable information about detector technology, shielding, and background mechanisms. CZT2 was the first array of pixellated CZT detectors, read out by an ASIC, to be flown on a balloon, and our results have demonstrated that the basic technical procedures envisioned for the EXIST concept are sound. The CZT1 data, while again proving the necessity of active shielding, provide further evidence that this shielding need not be of the heavy, inorganic scintillator type, but may rather be lighter plastic shielding to veto charged particles. This argues against prompt neutron reactions being a major source of background in CZT. The CZT2 spectra revealed no gamma-ray lines below 500 keV from activated isotopes, and the basic agreement with the CZT1 data and with simulations shows again that a combination of passive and plastic shielding can provide reasonable background levels. Our work on advanced CZT detectors for astronomical applications will continue with the development of CZT3, employing a 2×2 array of larger detectors with a more advanced contacting and readout scheme, as described separately in these proceedings.

ACKNOWLEDGMENTS

We would like to thank the entire NSBF team for a successful balloon flight, J. Apple and K. Dietz for technical support in the field, and B. Sundal for help with the VA-DAQ system. This work was supported in part by NASA grants NAG5-5103 and NAG5-5209.

REFERENCES

1. P. Bloser, T. Narita, J. Grindlay, and K. Shah, "Prototype imaging Cd-Zn-Te array detector," in *Semiconductors for Room-Temperature Radiation Detector Applications II*, R. James, T. Schlesinger, P. Siffert, M. Cuzin, M. Squillante, and W. Dusi, eds., *Proc. MRS* **487**, p. 153, 1998.
2. T. Narita, P. Bloser, J. Grindlay, R. Sudharsanan, C. Reiche, and C. Stenstrom, "Development of prototype pixellated PIN CdZnTe detectors," in *Hard x-ray and gamma-ray detector physics and applications*, F. P. Doty and R. B. Hoover, eds., *Proc. SPIE* **3446**, p. 218, 1998.
3. T. Narita, P. F. Bloser, J. E. Grindlay, J. A. Jenkins, and H. W. Yao, "Development of IMARAD CZT detectors with PIN contacts," in *Hard X-ray, Gamma-ray, and neutron detector physics*, R. B. James and R. C. Schirato, eds., *Proc. SPIE* **3768**, p. 55, 1999.
4. T. Narita, P. F. Bloser, J. E. Grindlay, and J. A. Jenkins, "Development of gold contacted flip-chip detectors with IMARAD CZT," in *Hard X-ray, Gamma-ray, and neutron detector physics II*, R. B. James and R. C. Schirato, eds., *Proc. SPIE* **4141**, p. 86, 2000.
5. S. D. Barthelmy, "Burst alert telescope (BAT) on the Swift MIDEX mission," in *X-ray and Gamma-ray Instrumentation for Astronomy XI*, K. A. Flanagan and O. H. W. Siegmund, eds., *Proc. SPIE* **4140**, 2000.
6. J. Grindlay and et al., "EXIST: a high sensitivity hard X-ray imaging sky survey mission for ISS," in *The Fifth Compton Symposium*, M. C. McConnell and J. M. Ryan, eds., *AIP Conf. Proc.* **510**, p. 784, 2000.
7. F. Harrison and et al., "Technology development for the Constellation-X hard x-ray telescope," in *EUV, X-ray, and Gamma-ray Instrumentation for Astronomy X*, O. H. W. Siegmund and K. A. Flanagan, eds., *Proc. SPIE* **3765**, p. 104, 1999.
8. T. J. O'Neill and et al., "The TIGRE gamma-ray telescope," in *The Fifth Compton Symposium*, M. C. McConnell and J. M. Ryan, eds., *AIP Conf. Proc.* **510**, p. 804, 2000.
9. P. Bloser, J. Grindlay, T. Narita, and F. Harrison, "CdZnTe background measurement at balloon altitudes with an active BGO shield," in *EUV, X-ray, and Gamma-ray Instrumentation for Astronomy IX*, O. H. W. Siegmund and M. Gummin, eds., *Proc. SPIE* **3445**, p. 186, 1998.
10. P. F. Bloser, J. E. Grindlay, T. Narita, and J. A. Jenkins, "Design and testing of a prototype pixellated CZT detector and shield for hard X-ray astronomy," in *EUV, X-ray, and Gamma-ray Instrumentation for Astronomy X*, O. H. W. Siegmund and K. A. Flanagan, eds., *Proc. SPIE* **3765**, p. 388, 1999.
11. P. F. Bloser, T. Narita, J. A. Jenkins, and J. E. Grindlay, "Construction and testing of a pixellated CZT detector and shield for a hard x-ray astronomy balloon flight," in *X-ray and Gamma-ray Instrumentation for Astronomy XI*, K. A. Flanagan and O. H. W. Siegmund, eds., *Proc. SPIE* **4140**, p. 237, 2000.
12. A. Parsons, S. Barthelmy, L. Bartlett, F. Birsa, N. Gehrels, J. Naya, J. Odom, S. Singh, C. Stahle, J. Tueller, and B. Teegarden, "CdZnTe background measurements at balloon altitudes," *Proc. SPIE* **2806**, p. 432, 1996.
13. F. Harrison, C. Hailey, J. Hong, A. Wong, and W. Cook, "Background in balloon-borne hard x-ray/soft gamma-ray cadmium zinc telluride detectors," *Nuc. Inst. Meth. A* , submitted.
14. K. Slavis, P. Dowkontt, F. Duttweiler, J. Epstein, P. Hink, G. Huszar, P. Leblanc, J. Matteson, R. Skelton, and E. Stephan, "High altitude balloon flight of CdZnTe detectors for high energy x-ray astronomy," in *EUV, X-ray, and Gamma-ray Instrumentation for Astronomy IX*, O. H. W. Siegmund and M. Gummin, eds., *Proc. SPIE* **3445**, p. 169, 1998.
15. K. Slavis, P. Dowkontt, F. Duttweiler, J. Epstein, P. Hink, G. Huszar, P. Leblanc, J. Matteson, R. Skelton, and E. Stephan, "High altitude balloon flight of CdZnTe detectors for high energy x-ray astronomy part ii," in *EUV, X-ray, and Gamma-ray Instrumentation for Astronomy X*, O. H. W. Siegmund and K. A. Flanagan, eds., *Proc. SPIE* **3765**, p. 388, 1999.
16. K. Slavis and et al., "Performance of a prototype CdZnTe detector module for hard x-ray astrophysics," in *X-ray and Gamma-ray Instrumentation for Astronomy XI*, K. A. Flanagan and O. H. W. Siegmund, eds., *Proc. SPIE* **4140**, p. 249, 2000.
17. P. Cheuvart, U. El-Hanany, D. Schneider, and R. Triboulet, "CdTe and CdZnTe crystal growth by horizontal Bridgman technique," *J. Crystal Growth* **101**, p. 270, 1990.
18. S. J. Sturner, H. Seifert, C. Shrader, and B. J. Teegarden, "MGEANT - a GEANT-based multi-purpose simulation package for gamma-ray astronomy missions," in *The Fifth Compton Symposium*, M. C. McConnell and J. M. Ryan, eds., *AIP Conf. Proc.* **510**, p. 814, 2000.

19. N. Gehrels, "Instrumental background in balloon-borne gamma-ray spectrometers and techniques for its reduction," *Nuc. Inst. Meth. A* **239**, p. 324, 1985.
20. D. A. Swartz, Y. Z. Chen, and B. D. Ramsey, "Background simulation for a balloon-borne gas scintillation proportional counter," in *X-ray and Gamma-ray Instrumentation for Astronomy XI*, K. A. Flanagan and O. H. W. Siegmund, eds., *Proc. SPIE* **4140**, 2000.
21. T. Armstrong, K. Chandler, and J. Barish, "Calculations of neutron flux spectra induced in the Earth's atmosphere by galactic cosmic rays," *J. Geophys. Res.* **78**, p. 2715, 1973.
22. K. Hecht, "Zum Mechanismus des Lichtelektrischen Primarstromes in Isolierenden Kristallen," *Zeits. Phys* **77**, pp. 235–243, 1932.